Algorithmic evaluation of lower jawbone segmentations

Jan Egger[a,b], Kerstin Hochegger[a], Markus Gall[a], Xiaojun Chen[c], Knut Reinbacher[d]
Katja Schwenzer-Zimmerer[d], Dieter Schmalstieg[a] and Jürgen Wallner[d]

[a] TU Graz, Institute for Computer Graphics and Vision, Inffeldgasse 16c/II, 8010 Graz, Austria
[b] BioTechMed-Graz, Krenngasse 37/1, 8010 Graz, Austria
[c] Shanghai Jiao Tong University, School of Mechanical Engineering, 800 Dong Chuan Road, Shanghai 200240, China
[d] Medical University of Graz, Department of Maxillofacial Surgery, Auenbruggerplatz 12, 8036 Graz, Austria

ABSTRACT

The lower jawbone (or mandible), is due to its exposure to complex biomechanical forces the largest and strongest facial bone in humans. In this publication, an algorithmic evaluation of lower jawbone segmentation with a cellular automata algorithm called GrowCut is presented. For an evaluation, the algorithmic segmentation results were compared with slice-by-slice segmentations from two specialized physicians, which is considered to assess the given ground truth. As a result, pure manual slice-by-slice outlining took on average 39 minutes (minimum 35 minutes and maximum 46 minutes). This stands in strong contrast to an algorithmic segmentation which needed only about one minute for an initialization, hence needing just a fraction of the manual contouring time. At the same time, the algorithmic segmentations could achieve an acceptable Dice Similarity Score (DSC) of nearly ninety percent when compared to the ground truth slice-by-slice segmentations generated by the physicians. This stands in direct comparison to somewhat above ninety percent Dice Score between the two manual segmentations of the jawbones. In summary, this contribution shows that an algorithmic GrowCut segmentation can be an alternative to the very time consuming manual slice-by-slice outlining in the clinical practice.

Keywords: Algorithm, Segmentation, Lower Jawbone, GrowCut, Dice Score.

1. DESCRIPTION OF PURPOSE

Facial defects and facial traumata including fractured bone segments are a common form of injury due to violent crimes, accidents or pathological processes. However, the most common form of facial injury are fractures of the mandible, which represent about 40% of all facial fractures [1]. Segmentation can provide two or three dimensional medical image analysis for localizing, quantifying and visualizing biological regions of interest in a great variety of structures (like the abdomen, the brain, the back) [2]-[25]. In that context, a digital capturing of the bone structures through (semi-)automatic segmentation can be very important for a better and faster assessment of the biological structure, morphology, diagnosis, treatment planning and production of patient individual implants [26]. Therefore, an algorithm supported segmentation is able to significantly shorten the operative planning and treatment time while in parallel improve the treatment quality [27], [28]. However – due to missing practical stable and inaccurate functions – automatic segmentations find no use in the daily clinical routine yet.

Others working in the field of (semi-)automatic jawbone segmentation are Barandiaran et al. [29] who presents the automatic segmentation and reconstruction of mandibular structures from Computed Tomography (CT) data. For the automatic segmentation process they establish a pipeline consisting of several threshold filters. Amongst others, they apply the multiple threshold method by Otsu [30]. Harandi et al. [31] introduce upper and lower jaw segmentation in dental x-ray images using a modified Active Contour [32]. In a first step, they separate the upper and lower jaw, followed by a modified geodesic active contour and morphological operations. The automatic segmentation of mandibles in low-dose CT data is demonstrated by Lamecker et al. [33]. For an automatic segmentation in low-dose images, their work explores the ability of a model-based segmentation using a 3D statistical mandible model. The method consists of a training and a segmentation phase and includes a deformation strategy for detecting the mandibular bone. A segmentation approach to extract the trabecular jawbone in cone beam CT (CBCT) data sets is studied by Nackaerts et al. [34]. In summary, they used adaptive thresholding for the automatic segmentation of upper and lower jaws. For testing two volumes of interest each jaw were manually delineated and micro-CT images served as high-resolution ground truth images. Tan et al. [35] present threshold segmentations in 3D reconstructions of mandible CT images. To obtain an approximate segmentation result they used dilation operations, and a more precise segmentation results was achieved with the additional help of logical operations and region growing. Kainmueller and colleagues [36] performed the automatic extraction of mandibular nerve and bone from cone-beam CT data. The fully-automatic method is based on a combined statistical shape model [37] of the nerve and the bone and a Dijkstra-based [38] optimization procedure.

Medical Imaging 2017: Biomedical Applications in Molecular, Structural, and Functional Imaging
edited by Andrzej Krol, Barjor Gimi, Proc. of SPIE Vol. 10137, 101370C · © 2017 SPIE
CCC code: 1605-7422/17/$18 · doi: 10.1117/12.2249532

Furthermore, Koningsveld [39] presents the automated segmentation of the mandibular nerve canal in CBCT images in his thesis. The approach begins with a combination of a smoothing and gradient filter to reduce noise and enhance the edges of the canal, which prepares the image for a fuzzy-connectedness method. Finally, the results are interpolated to fill in gaps and correct any errors. However, to the best of our knowledge, there is no work that has studied the semi-automatic segmentation of the lower jawbone in CT images with GrowCut. Moreover, and in contrast to the existing works, the GrowCut algorithm is publicly available and can be used by other groups without having to re-implement the algorithm. In this study the accurate function of the semi-automatic algorithm GrowCut is assessed for a practical use in the clinical routine. In that context the algorithm is objectively compared to a ground truth segmentation of lower jaw data sets using a prospective randomized study design.

This contribution is organized as follows: Section 2 introduces details of the methods, Section 3 presents experimental results and Section 4 concludes the paper and gives an outlook on future work.

2. METHODS

For this study, twenty high-resolution (512x512) Computed Tomography (CT) data sets with physiologic, complete, mandibular bone structures without teeth have been selected. However, incomplete data sets consisting of mandibular structures altered by iatrogenic or pathological factors or fractured mandibles were excluded from the study. All data sets were acquired within a nine month period in the clinical routine out of diagnosis and treatment reasons. Furthermore, ten data sets were selected in a randomization process by a computer program (Randomizer®; https://www.randomizer.at). To provide an objective and clear bone structure assessment for the manual segmentation (ground truth), physiologic non-altered mandibles were used for this trial. For an algorithm supported segmentation, the user had to initialize the GrowCut [40] approach by marking parts of the mandibular bone and the background in axial, sagittal and coronal slices, respectively. This course of action is similar to previous studies for glioblastoma multiforme (GBM) and pituitary adenomas (PA) [41], [42]. However, in the previous works, the tumors could be segmented by initializing on three slices only, however, for an acceptable automatic segmentation of the lower jawbone, six slices had to be initialized for a satisfying segmentation result. Like shown in Figure 1, for three slices the fore- (green) and background (yellow) had to be initialized in an axial, sagittal and coronal slice around the anterior mandible (symphysis / para-symphysis). And like shown in Figure 2, another fore- (green) and background (yellow) initialization of GrowCut had to be performed in an axial, sagittal and coronal slice around parts of the cranial mandible (condyle and processus). Nevertheless, a user trained in this initialization task was still able to perform it in around one minute and afterwards the user had just to trigger the algorithmic segmentation process. Finally, the automatic segmentation results could be saved by the user as a 3D mask, which was used for statistical analysis in comparison to the manual generated ground truth segmentations done by two specialized physicians. To generate the ground truth segmentations, we set up a prototype with simple slice-by-slice contouring capabilities under MeVisLab [43]. This software was used by two physicians to outline the mandibular bones in the patients CT data in axial directions. Besides, the times were measured, starting with loading a dataset and ending with saving the single contours as one binary 3D mask.

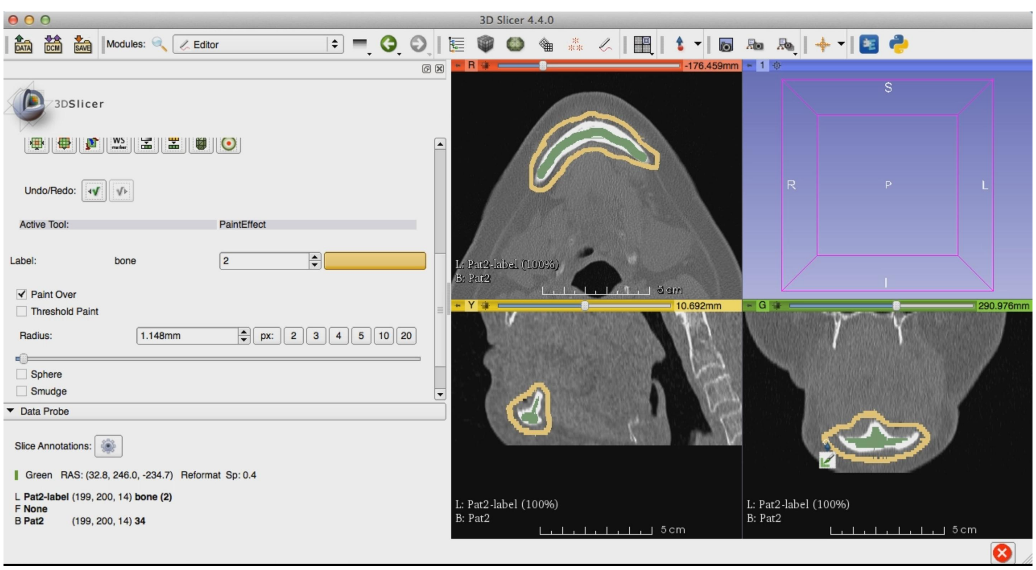

Fig. 1: Fore- (green) and background (yellow) initialization of GrowCut in the lower jawbone in an axial, sagittal and coronal slice around the anterior mandible (symphysis / para-symphysis).

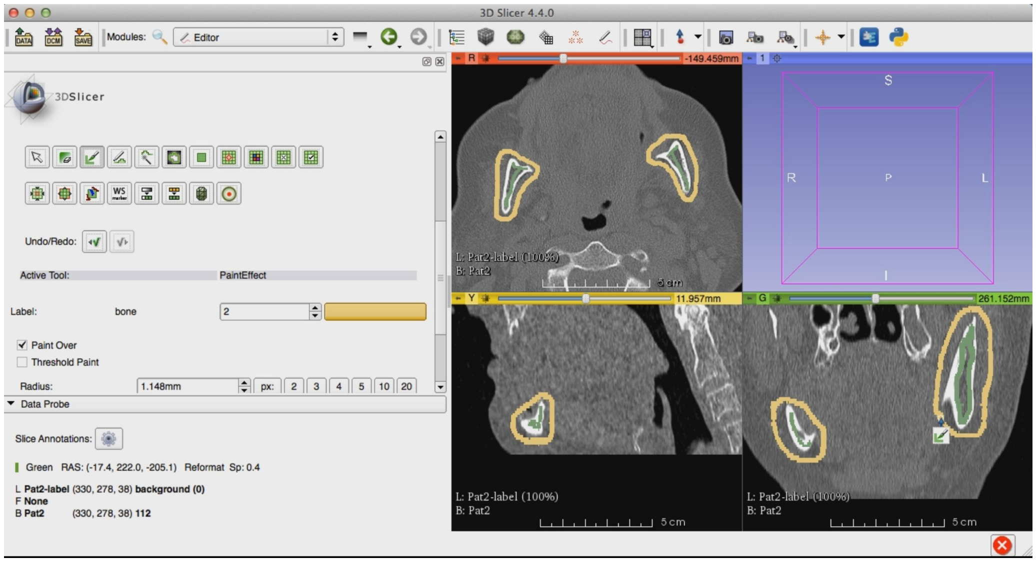

Fig. 2: Fore- (green) and background (yellow) initialization of GrowCut in the lower jawbone in an axial, sagittal and coronal slice around parts of the mandible.

3. RESULTS

Overall, the goal of this study was to investigate the feasibility of an algorithm-supported jawbone segmentation for the clinical practice. In doing so, two metrics were used for an in-depth evaluation of the GrowCut algorithm: the agreement between two segmentations (manual/manual and manual/algorithmic), expressed as Dice Score [44], and the segmentation times (manual and algorithmic). As result, the agreement between two manual segmentations yielded to a Dice Score of 93.61±0.98% and the agreement between a manual and an automatic segmentation yielded to a Dice Score of 85.46±3.38%. Table 1 depicts the summary of the results, consisting of the minimum (Min.), the maximum, (Max.) the mean μ and the standard deviation σ for all lower jawbone segmentations (manual and algorithmic).

	Volumes of the Lower Jawbones (cm^3)			Dice Scores (%)	Manual Segmentation Times in Minutes	
	Physician a	Physician b	Algorithmic	Physician a / Algorithmic	Physician a	Physician b
Min.	17.33	17.73	16.55	80.73	36	35
Max.	46.51	47.51	52.09	90.33	46	42
$\mu \pm \sigma$	31.28 ± 10.69	31.35 ± 10.59	32.18 ± 13.02	85.46 ± 3.38	38.6 ± 3.31	38.4 ± 2.27

Tab. 1: Summary of segmentation results: Min., Max., mean μ and standard deviation σ for ten lower jawbones.

For visual inspection, Figure 3 presents the results of two manual segmentations (blue and green) and a manual segmentation superimposed into a patient's 3D visualization (white and orange). Figure 4 on the other hand, presents the results of a manual (white) and an automatic (gold) segmentation. Moreover, the automatic segmentation result has been superimposed into a 3D visualization of the patient's skull (gold and gray) on the right side of Figure 4. Note that some initial results have been presented and discussed as a talk [45] at the 20th Annual Congress of the Austrian Society of Oral and Maxillofacial Surgery (ÖGMKG), in Bad Hofgastein, Salzburg, Austria, and as a late breaking research poster [46] at the 38th Annual International Conference of the IEEE Engineering in Medicine and Biology Society (EMBC) in Orlando, FL, USA. However, at the ÖGMKG congress we showed only some first outcomes of the segmentation results and at the EMBC we presented only a one page summarized description of the algorithm. All statistical results and a precise description of the methods are only presented in full details within this contribution.

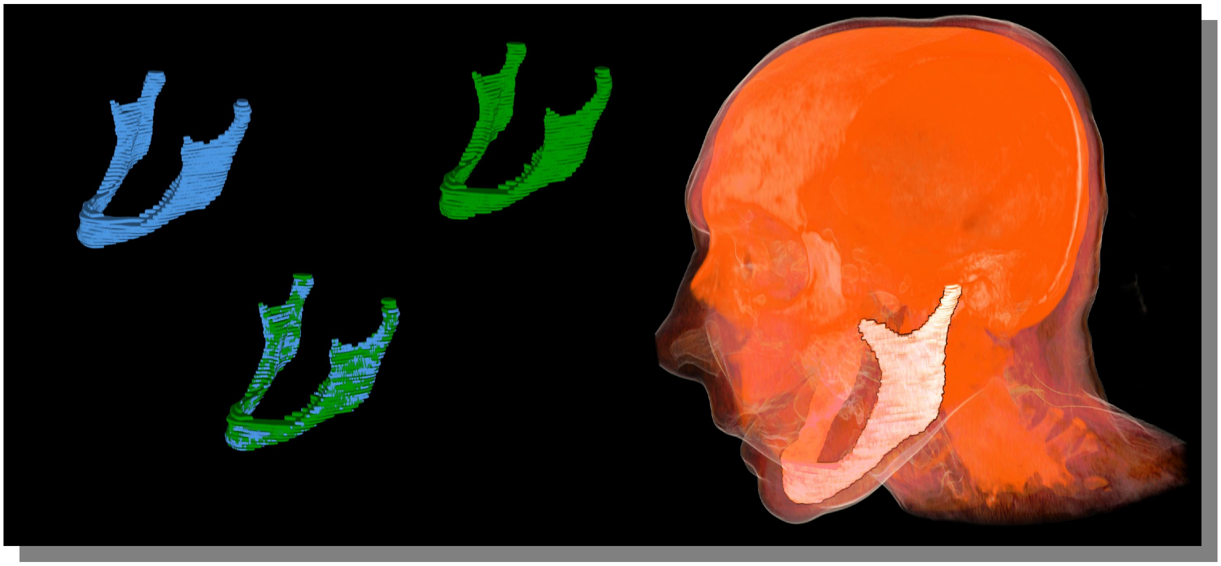

Fig. 3: Manual/Manual segmentation results for visual inspection. The segmentation results of two manual segmentations (blue and green) are shown, including a superimposed visualization of the automatic segmentation (white) into a patient's 3D visualization (orange).

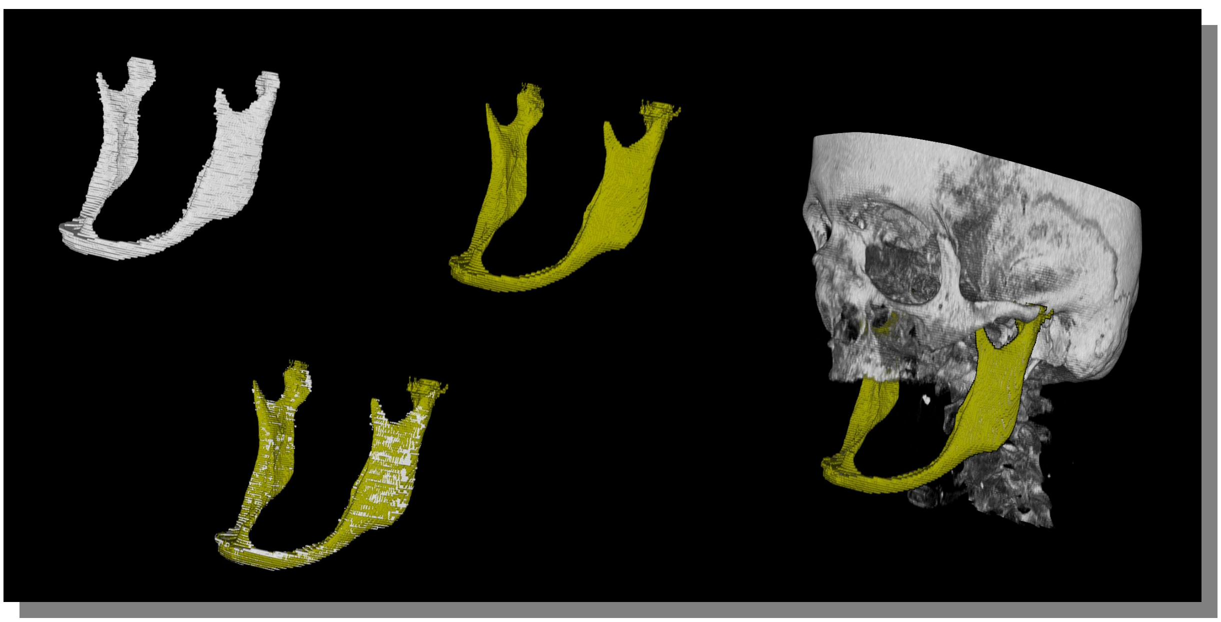

Fig. 4: Manual/Algorithmic segmentation results for visual inspection. A manual (white) and automatic (gold) segmentation result is presented, including a superimposed visualization of the automatic segmentation (gold) into a 3D visualization of the patient's skull (gray).

4. CONCLUSIONS

In this contribution, the algorithmic segmentation of the lower jawbone with a semi-automatic cellular automata algorithm called GrowCut has been studied for clinical evaluation and was set in comparison to a slice by slice generated ground truth. For the semi-automatic segmentation the user marked parts of the mandibular bone and the background in axial, sagittal and coronal slices, similar as it was already performed for a GrowCut-based segmentation on other anatomical structures in earlier investigations [41], [42]. A trained user could achieve this initialization in approximately a minute, which was followed by the successfully performed automatic segmentation process of the algorithm. Finally, the results were saved as 3D mask for further statistical analysis with the ground truth segmentations from two physicians. In a nutshell, satisfying qualitative and quantitative segmentation results could be achieved with the algorithmic support in a much shorter time. High Dice Score values were achieved when comparing the semi-automatic to the manual slice by slice segmentation which means that the cellular automata algorithm provides a quite high accuracy in the segmentation process. Hence, the results of this study demonstrated a more efficient alternative course of action in lower jawbone volumetry compared to the very time consuming pure manual slice-by-slice outlining. Due to its stable, accurate and time saving function in the practical use the semi-automatic segmentation method investigated in this study could be used in the clinical routine and support e.g. the planning of operations or the creation of 3D models in maxillofacial surgery for a higher quality in the further operative treatment. Further, the used algorithm is due to its open source basis available to the public and gives herewith the opportunity for a further development by other groups without the disadvantages of limiting monetary aspects or license agreements.

There are several areas for future work, in particular the evaluation of this algorithm with a greater amount of data and with other facial bones as also the comparison with other freely available segmentation methods like the robust statistics segmentation (RSS) algorithm. Moreover, using the segmentation results to support computer-aided reconstruction of facial defects [47], including a surgical template design for oral implantology [48] and furthermore importing the results into a surgical navigation system based on augmented reality (AR) [49], [50] (www.augmentedrealitybook.org) using an optical see-through head-mounted display [51]. Finally, applying the algorithm to other medical data and structures like the aorta [52]-[54] and use the segmentation result to calculate the centerline of the vessel [55] and simulate a stent [56]-[58].

ACKNOWLEDGEMENT

The work received funding from BioTechMed-Graz ("*Hardware accelerated intelligent medical imaging*") and the 6^{th} Call of the Initial Funding Program from the Research & Technology House (F&T-Haus) at the Graz University of Technology ("*Interactive Planning and Reconstruction of Facial Defects*", PI: DDr. Jan Egger). Dr. Chen receives support by the Natural Science Foundation of China (Grant No.: 81511130089) and the Foundation of Science and Technology Commission of Shanghai Municipality (Grants No.: 14441901002, 15510722200 and 16441908400). A video tutorial of the segmentation workflow can be found under the following YouTube channel:

https://www.youtube.com/c/JanEgger/videos

REFERENCES

[1] Chrcanovic, B. R. "Fixation of mandibular angle fractures: in vitro biomechanical assessments and computer-based studies," Oral Maxillofac Surg., 17(4), 251-68 (2013).
[2] Lu, J. et al. "Detection and visualization of endoleaks in CT data for monitoring of thoracic and abdominal aortic aneurysm stents," Proceedings of SPIE Medical Imaging Conference, Vol. 6918, pp. 69181F(1-7), San Diego, USA, (2008).
[3] Egger, J. et al "Interactive Volumetry of Liver Ablation Zones," Sci Rep 5:15373 (2015).
[4] Greiner, K. et al. "Segmentation of Aortic Aneurysms in CTA Images with the Statistic Approach of the Active Appearance Models," Proceedings of Bildverarbeitung für die Medizin (BVM), Berlin, Germany, Springer Press, pages 51-55 (2008).
[5] Egger, J. et al. "Nugget-Cut: A Segmentation Scheme for Spherically- and Elliptically-Shaped 3D Objects," 32nd Annual Symposium of the German Association for Pattern Recognition (DAGM), LNCS 6376, pp. 383–392, Springer Press, Darmstadt, Germany (2010).
[6] Egger, J. et al. "Manual refinement system for graph-based segmentation results in the medical domain," Journal of medical systems 36(5), 2829-2839 (2012).
[7] Egger, J. et al. "Template-Cut: A Pattern-Based Segmentation Paradigm," Sci Rep 2:420 (2012).
[8] Kuhnt, D. et al. "Fiber tractography based on diffusion tensor imaging compared with high-angular-resolution diffusion imaging with compressed sensing: initial experience," Neurosurgery, 72(0 1): 165-175 (2013).
[9] Egger, J. et al. "Pituitary Adenoma Segmentation," In: Proceedings of International Biosignal Processing Conference, Charité, Berlin, Germany (2010).
[10] Egger, J. et al "A flexible semi-automatic approach for glioblastoma multiforme segmentation," Proceedings of International Biosignal Processing Conference, Charité, Berlin, Germany (2010).
[11] Egger, J. et al. "Preoperative Measurement of Aneurysms and Stenosis and Stent-Simulation for Endovascular Treatment," IEEE International Symposium on Biomedical Imaging: From Nano to Macro, Washington (D.C.), USA, pp. 392-395, IEEE Press (2007).
[12] Zukic, D. et al. "Segmentation of Vertebral Bodies in MR Images," Vision, Modeling, and Visualization (VMV), The Eurographics Association, pp. 135-142, (2012).

[13] Zukic, D. et al. "Robust Detection and Segmentation for Diagnosis of Vertebral Diseases using Routine MR Images," Computer Graphics Forum, Volume 33, Issue 6, Pages 190–204 (2014).
[14] Egger, J. et al. "PCG-Cut: Graph Driven Segmentation of the Prostate Central Gland," PLOS ONE 8 (10), e76645 (2013).
[15] Egger, J. et al. "A Comparison of Two Human Brain Tumor Segmentation Methods for MRI Data," Proceedings of 6th RB Conference on Bio-Medical Engineering, State Technical University, Moscow, Russia, 4 pages (2010).
[16] Zukić, D. et al. "Glioblastoma Multiforme Segmentation in MRI Data with a Balloon Inflation Approach," Proceedings of 6th RB Conference on Bio-Medical Engineering, State Technical University, Moscow, Russia, pp. 4 pages (2010).
[17] Schwarzenberg, R. et al. "A Cube-Based Approach to Segment Vertebrae in MRI-Acquisitions," Proceedings of Bildverarbeitung für die Medizin (BVM), Springer Press, pp. 69-74 (2013).
[18] Egger, J. et al. "A medical software system for volumetric analysis of cerebral pathologies in magnetic resonance imaging (MRI) data," Journal of medical systems 36 (4), 2097-2109 (2012).
[19] Schwarzenberg, R. et al. "Cube-Cut: Vertebral Body Segmentation in MRI-Data through Cubic-Shaped Divergences," In: PLoS One (2014).
[20] Egger, J. et al. "Square-cut: a segmentation algorithm on the basis of a rectangle shape," PLoS One 7, e31064; DOI:10.1371/journal.pone.0031064 (2012).
[21] Egger, J. "Refinement-Cut: User-Guided Segmentation Algorithm for Translational Science," Sci Rep 4:5164 (2014).
[22] Steger, S. and Sakas, G. "FIST: Fast Interactive Segmentation of Tumors," Abdominal Imaging, Springer, pp. 125-132 (2011).
[23] Bauer, M. et al. "A fast and robust graph-based approach for boundary estimation of fiber bundles relying on fractional anisotropy maps," 20th International Conference on Pattern Recognition (ICPR), Istanbul, Turkey, pp. 4016-4019 (2010).
[24] Bauer, M. et al. "Boundary estimation of fiber bundles derived from diffusion tensor images," International journal of computer assisted radiology and surgery 6 (1), 1-11 (2011).
[25] Egger, J. et al. "Interactive-cut: Real-time feedback segmentation for translational research," Computerized Medical Imaging and Graphics 38 (4), 285-295 (2014).
[26] Schvartzman, S. C. et al., "Computer-aided trauma simulation system with haptic feedback is easy and fast for oral-maxillofacial surgeons to learn and use," J Oral Maxillofac Surg., 72(10), 1984-93 (2014).
[27] Zinser, M. J. et al., "Computer-assisted orthognathic surgery: waferless maxillary positioning, versatility, and accuracy of an image-guided visualisation display," Br J Oral Maxillofac Surg. 51(8), 827-33 (2013).
[28] Tucker, S., Cevidanes, L. H., Styner, M., Kim, H., Reyes, M., Proffit, W., Turvey, T. Comparison of actual surgical outcomes and 3-dimensional surgical simulations. J Oral Maxillofac Surg. 2010 Oct;68(10), 2412-21 (2010).
[29] Barandiaran, I. et al. "An automatic segmentation and reconstruction of mandibular structures from CT-data," Proceedings of the 10th international conference on Intelligent data engineering and automated learning, Springer Press, 649-655 (2009).
[30] Otsu, N. "A threshold selection method from gray-level histogram," IEEE Trans. Syst. Man Cybern., 9, 62-66 (1976).
[31] Harandi, A. A. et al. "Upper and Lower Jaw Segmentation in Dental X-ray Image Using Modified Active Contour," International Conference on Intelligent Computation and Bio-Medical Instrumentation, 124-127 (2011).
[32] Kass, M. et al. "Snakes - Active Contour Models," International Journal of Computer Vision, 1(4), 321-331 (1987)
[33] Lamecker, H. et al. "Automatic Segmentation of Mandibles in Low-Dose CT-Data," Int. J. Computer Assisted Radiology and Surgery, 1(1), 393-395 (2006).
[34] Nackaerts, O. et al. "Segmentation of Trabecular Jaw Bone on Cone Beam CT Datasets," Clin Implant Dent Relat Res. 2015 Dec;17(6), 1082-91 (2015).
[35] Tan, P. Y. et al. Improving Threshold Segmentation in 3D Reconstruction of Mandible CT Image. Journal of Sichuan University. Medical science edition, 46(3), 458-62 (2015).
[36] Kainmueller, D. et al. "Automatic Extraction of Mandibular Nerve and Bone from Cone-Beam CT Data," Med Image Comput Comput Assist Interv. 2009;12(Pt 2), 76-83 (2009).
[37] Cootes, T. F. et al. "Active Shape Models - Their Training and Application," Comput. Vis. Image Underst. 61(1), 38-59 (1995)
[38] Dijkstra, E. W. "A note on two problems in connexion with graphs," Num. Math. 1, 269-271 (1959).
[39] Koningsveld, A. "Automated Segmentation of the Mandibular Nerve Canal in CBCT images," Master Thesis Faculty of Engineering Technology, Campus De Nayer, KU Leuven, 1-68 (2014).
[40] Vezhnevets, V., Konouchine, V. "GrowCut-Interactive multi-label N-D image segmentation," Proc Graphicon, 150-156 (2005)
[41] Egger, J. et al. "GBM Volumetry using the 3D Slicer Medical Image Computing Platform," Sci Rep., NPG, 3:1364, 1-7 (2013)
[42] Egger, J. et al. "Pituitary Adenoma Volumetry with 3D Slicer," PLoS ONE 7(12), e51788 (2012).
[43] Egger, J. et al. "Integration of the OpenIGTLink Network Protocol for Image-Guided Therapy with the Medical Platform MeVisLab," Int J Med Robot., 8(3), 282-90 (2012).
[44] Sampat, M. P. et al. "Measuring Intra- and Inter-Observer Agreement in Identifying and Localizing Structures in Medical Images," IEEE International Conference on Image Processing, 81-84 (2006).
[45] Wallner, J. et al "Image-guided real-time-segmentation of the mandibular bone: Can a simple Segmentation approach provide a satisfying result for a practicable use?," 20th Annual Congress of the Austrian Society of Oral and Maxillofacial Surgery (ÖGMKG), V15, Spa- and Convention Center, Bad Hofgastein, Salzburg, Austria, (2016).
[46] Egger, J. et al. "Clinical Evaluation of Mandibular Bone Segmentation," IEEE Engineering in Medicine and Biology Society (EMBC'16), Late breaking Research Posters Paper, Orlando, FL, USA (2016).

[47] Gall, M. et al. "Computer-aided Reconstruction of Facial Defects," IEEE Engineering in Medicine and Biology Society (EMBC'16), Late breaking Research Posters Paper, Orlando, FL, USA (2016).
[48] Chen, X., et al. "A semi-automatic computer-aided method for surgical template design," Sci. Rep. 6, 20280, 1-18 (2016)
[49] Reinbacher, K. et al. "AR (Augmented Reality)-Paradigm shift in the Therapy Design," 20th Annual Congress of the Austrian Society of Oral and Maxillofacial Surgery (ÖGMKG), V78, Spa- and Convention Center, Bad Hofgastein, Austria (2016)
[50] Schmalstieg, D., Höllerer, T. "Augmented Reality: Principles and Practice," Addison-Wesley Professional; 1st ed., Paperback, 528 pages, ISBN 978-0321883575, https://arbook.icg.tugraz.at/ (2016).
[51] Chen, X. et al. "Development of a Surgical Navigation System based on Augmented Reality using an Optical see-through Head-mounted Display," J Biomed Inform. 2015 Jun;55, 124-31 (2015).
[52] Renapurkar, R. D. et al. "Aortic volume as an indicator of disease progression in patients with untreated infrarenal abdominal aneurysm," European Journal of Radiology 81 (2012) e87–e93 (2012).
[53] Egger, J. et al. "Graph-Based Tracking Method for Aortic Thrombus Segmentation," Proceedings of 4th European Congress for Medical and Biomedical Engineering, Engineering for Health, Antwerp, Belgium, Springer, pp. 584-587 (2008).
[54] Egger, J. et al. "Aorta Segmentation for Stent Simulation," 12th International Conference on Medical Image Computing and Computer Assisted Intervention (MICCAI), Cardiovascular Interventional Imaging and Biophysical Modelling Workshop, 10 pages, London, UK (2009).
[55] Egger, J., Mostarkic, Z., Grosskopf, S. and Freisleben, B. "A Fast Vessel Centerline Extraction Algorithm for Catheter Simulation," 20th IEEE International Symposium on Computer-Based Medical Systems, Maribor, Slovenia, pp. 177-182, IEEE Press (2007).
[56] Egger, J. et al. "Simulation of bifurcated stent grafts to treat abdominal aortic aneurysms (AAA)," Proceedings of SPIE Medical Imaging Conference, Vol. 6509, pp. 65091N(1-6), San Diego, USA (2007).
[57] Egger, J. et al. "Fast self-collision detection and simulation of bifurcated stents to treat abdominal aortic aneurysms (AAA)," 29th Annual International Conference of the IEEE Engineering in Medicine and Biology Society, Lyon, France, pp. 6231-6234, IEEE Press (2007).
[58] Egger, J. et al. "Modeling and Visualization Techniques for Virtual Stenting of Aneurysms and Stenoses," Computerized Medical Imaging and Graphics, 36(3), pp. 183-203 (2012).